

FRACTAL STRUCTURES DRIVEN by SELF-GRAVITY: Molecular clouds and the Universe

Francoise Combes
Observatoire de Paris, DEMIRM
 61 Av. de l'Observatoire, F-75014 Paris, FRANCE

1. Introduction: Fractal Concepts

Fractals have been introduced by Mandelbrot (1975) to define geometrical ensembles, or mathematical sets, that have a fractional dimension. He pioneered the study of very irregular mathematical sets, where the methods of classical calculus cannot be applied. Fractals are not smooth nor differentiable; they are characterized by self-similarity. Their geometrical structure has details at all scales, and the details are representative of the whole.

Fractals are very rich, since they give the best approximation for many natural phenomena, that cannot be represented by regular and smooth geometries (natural systems are only fractal between two boundaries, with upper and lower cut-offs, and not true mathematical fractals, of course). There can exist a large part of randomness in fractals, and the fractal dimension and exponents of scaling laws are the tools to quantify the hidden order in them.

There are many definitions of the dimension, trying to quantify how much space a system fills. We will use mainly the Hausdorff dimension D , based on the Hausdorff measure, that generalizes the notion of length, area and volume. When the length scale is magnified by λ , a regular and smooth set's area and volume are respectively scaled by λ^2 , λ^3 , while the fractal set measure is scaled by λ^D . For the astrophysical systems that we describe below, the mass contained within a scale r is $M \propto r^D$, with D a fractional number between 1 and 3.

2. Interstellar Clouds

The gaseous medium pervading the galaxy in between stars is highly structured. This medium consists of clouds of hydrogen, either atomic or molecular, according to its density or column density. A quick look at



the Milky Way reveals at once the very irregular and clumpy structure of the interstellar medium (ISM), while the stellar distribution is much smoother. Sizes of the clouds range from 100pc (the so-called Giant Molecular Clouds or GMC) down to 20 AU the smallest structures observed through VLBI in the vicinity of the Sun, in absorption in front of quasars (e.g. Davis et al 1996). This corresponds to 6 orders of magnitude in size, and about 10 in masses.

The geometrical appearance is very irregular, but can be characterized by sheets and filaments of great contrast. The aspect is self-similar, which can be glanced from clouds in the Galaxy at very different distances from the Sun. The dynamics of the ISM has always been mysterious, since it was expected that clouds collapse in a few million years to form stars. But molecular clouds, at all scales, are found to be relatively stable over times long compared to the free-fall time of the cloud at the given scale.

2.1. SCALING LAWS

The various structures of interstellar clouds are not distributed at random, but obey power-law relations between size, linewidth and mass (cf Larson 1981). These power-laws demonstrate the self-similar nature, and the scaling properties of the ISM: no peculiar scale exists (except at the two boundaries of course, lower and upper cut-offs). The mass of the clouds is always a very uncertain quantity to obtain, since there is no good universal tracer. The H_2 molecule does not radiate in the cold conditions of the bulk of the ISM (10-15 K), since it is symmetric, with no dipole moment. The first tracer is the most abundant molecule CO (10^{-4} with respect to H_2), but it is most of the time optically thick, or photo-dissociated (cf below). More direct quantities to measure are the sizes R and the line-widths or velocity dispersion σ , and the two are linked through a power-law relation:

$$\sigma \propto R^q$$

with q between 0.3 and 0.5 (e.g. Larson 1981, Scalo 1985, Solomon et al 1987, cf 1). Besides, molecular clouds appear to be virialised (at least within the uncertainties of mass determination) over all scales, so that

$$\sigma^2 \propto M/R$$

and the size-mass relation follows:

$$M \propto R^D$$

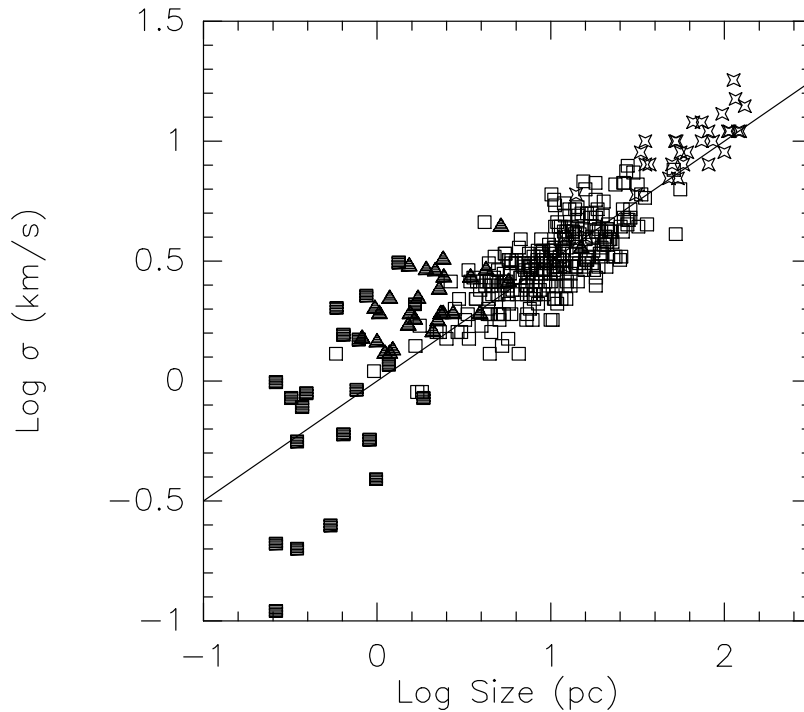


Figure 1. Size-linewidth relation taken from Solomon et al (1987) for the empty squares, from Dame et al (1986) for the empty stars, from Heithausen (1996) for the filled triangles, and from Magnani et al (1985) for the filled squares. The two latter samples concern high latitude molecular clouds.

with D the Hausdorff fractal dimension between 1.6 and 2. It can be deduced also that the mean density over a given scale R decreases as $1/R^\alpha$, where α is between 1 and 1.4.

2.2. HIERARCHICAL AND TREE INTERPRETATIONS

The observations of molecular clouds reveal that the structure is highly hierarchical, smaller clumps being embedded within the larger ones. Is this a completely exclusive relation, or are there isolated clumps? This is difficult to disentangle, since we have no real 3D picture of the ISM, the third dimension being traced by the radial velocity, and the latter being turbulent and not systematic. It has been possible, however, to build a tree structure where each clump has a parent for instance for clouds in Taurus, a very nearby region (Houlahan & Scalo 1992).

This recursive structure might tell us about the formation mechanism, as will be detailed later on. Basically, if self-gravity is the dominant force, density contrast will be built through Jeans instability, and this is a recursive process, in a quasi isothermal medium. The cooling is very efficient in the dense ISM, and it can be considered almost isothermal.

2.3. FRACTAL DIMENSIONS

There are various ways to quantify the observed self-similarity, and to define fractal dimensions. One of them is just to measure in 2D the surface versus the perimeter of a given structure. This method has been used in 2D maps, like the IRAS continuum flux, or the extinctions maps of the sky. In all cases, this method converges towards the same fractal dimension D_2 . For a curve of fractal dimension D_2 in a plane, the perimeter P and area A are related by

$$P \propto A^{D_2/2}$$

Falgarone et al (1991) find a dimension $D_2 = 1.36$ for CO contours both at very large (degrees) and very small scales (arcmin), and the same is found for IRAS 100μ contours in many circumstances (e.g. Bazell & Desert 1988). Comparable dimensions (D_2 between 1.3 and 1.5) are found with any tracer, for instance HI clouds (Vogelaar & Wakker 1994).

Note that the projection of a fractal of dimension D is not mandatorily a fractal, but if it is one with dimension D_p it is impossible a priori to deduce its fractal dimensions, except that

$$\begin{aligned} D_p &= D \text{ if } D \leq 2 \\ D_p &= 2 \text{ if } D \geq 2 \end{aligned}$$

(Falconer 1990).

2.4. TECHNICAL BIASES

It is a very difficult task to trace quantitatively the fractal structure of the ISM. Dense gas is molecular, and cold H_2 molecules do not radiate (Combes & Pfenniger 1997). The trace molecules such as CO are either optically thick, or not thermally excited (in low-density regions), or photo-dissociated near ionizing stars. The large range of scales is also a source of bias: the small scales are not resolved, and observed maps are smoothed out. This process, which confuses the fractal with a diffuse medium of fractal dimension 3, can lead to underestimates of the mass by factors more than 10 (e.g. simulations in Pfenniger & Combes 1994).

The mass spectrum of density fluctuations has often been studied as another way to characterise the ISM structure, and may be also to predict the mass spectrum of stars that form within these clouds. The differential mass spectrum dN/dm has been found to obey a power-law

$$dN/dm \propto m^\gamma$$

with $\gamma = -1.5 \pm 0.2$, between masses of 1 to $10^6 M_\odot$ (Casoli et al 1984, Solomon et al 1987, Brand & Wouterloot 1995). But this result has been obtained through molecular lines surveys. When extinction surveys are used, to determine a size spectrum (that can be directly related to the mass spectrum), a much flatter power law is found, and this has been attributed to occlusion (Scalo & Lazarian 1996), i.e. due to blocking of clouds by larger foreground clouds. Although this affects much less spectral studies, there could also be occlusion at a given velocity.

More recently, Heithausen et al (1998) have extended this relation over 5 orders of magnitudes in masses, down to Jupiter masses, and they found a steeper slope $\gamma = -1.84$. Their mass-size relation is $M \propto r^{2.31}$, also much steeper than previous studies, but the estimation of masses at small scales is quite uncertain (in particular the conversion factor between CO and H₂ mass could be much higher).

2.5. TURBULENCE

Everybody agrees that the word characterising the best the ISM is "turbulence". In laboratory it is well known that a laminar flow can turn turbulent when the Reynolds number is larger than a critical value, i.e.

$$Re = vl/\nu > R_c$$

where v is the velocity, l a typical dimension, and ν the kinematic viscosity. This means that the advection term $\mathbf{v} \cdot \nabla \mathbf{v}$ dominates the viscous term in the fluid equation. The turbulent state is characterised by unpredictable fluctuations in density and pressure, and a cascade of whirls. In the ISM, the viscosity can be estimated from the product of the macroturbulent velocity (or dispersion) and the mean-free-path of cloud-cloud collisions (since the molecular viscosity is negligible). But then the Reynolds number is huge ($\approx 10^9$), and the presence of turbulence is not a surprise.

This fact has encouraged many interpretations of the ISM structure in terms of what we know from incompressible turbulence. In particular, the Larson relations have been found as a sign of the Kolmogorov cascade (Kolmogorov 1941). In this picture, energy is dissipated into heat only at the lower scales, while it is injected only at large scale, and

transferred all along the hierarchy of scales. Writing that the energy transfer rate $v^2/(r/v)$ is constant gives the relation

$$v \propto r^{1/3}$$

which is close to the observed scaling law, at least for the smallest cores (Myers 1983). The source of energy at large scale would then be the differential galactic rotation and shear (Fleck 1981). This idealized view has been debated (e.g. Scalo 1987): it is not obvious that the energy cascades down without any dissipation in route (or injection), given the large-scale shocks, flows, winds, etc... observed in the ISM. Also, the interstellar medium is highly compressible, and its behaviour could be quite different from ordinary liquids in laboratory.

Besides, many features of ordinary turbulence are present in the ISM. For instance, Falgarone et al (1991) have pointed out that the existence of non-gaussian wings in molecular line profiles might be the signature of the intermittency of the velocity field in turbulent flows. More precisely, the ^{13}CO average velocity profiles have often nearly exponential tails, as shown by the velocity derivatives in experiments of incompressible turbulence (Miesch & Scalo 1995). Comparisons with simulations of compressible gas give similar results (Falgarone et al 1994). Also the curves obtained through 2D slicing of turbulent flows have the same fractal properties as the 2D projected images of the ISM; their fractal dimension D_2 obtained from the perimeter-area relation is also 1.36 (Sreenivasan & Méneveau 1986).

More essential, the ISM is governed by strong fluctuations in density and velocity. It appears chaotic, since it obeys highly non-linear hydrodynamic equations, and there is coupling of phenomena at all scales. This is also related to the sensibility to initial conditions that defines a chaotic system. The chaos is not synonymous of random disorder, there is a remarquable ordering, which is reflected in the scaling laws. The self-similarity over several orders of magnitude in scale and mass means also that the correlation functions behave as power-laws, and that there is no finite correlation length. This characterizes critical media, experiencing a second order phase transition for example. This analogy will be developed further in this chapter.

2.6. SELF-GRAVITY

Although the ISM is a self-organizing, multi-scale medium, comparable to what is found in laboratory turbulence, there are very special particularities that are not seen but in astrophysics. Self-gravity is a dominant, while it has not to be considered in atmospheric clouds for

instance. It has been recognized by Larson (1981) and by many others that at each scale the kinetic energy associated with the linewidths balances the gravitational energy: clouds are virialized approximately, given their very irregular geometry.

This property of course has to stop at the largest scale, when the influence of the galactic gravity, and associated shear, intervenes. This scale is that of the Giant Molecular Clouds, of the order of 100pc in size, and $10^6 M_{\odot}$ in mass. They are the largest self-gravitating structures in the Galaxy. At the other extremity, the smallest scales are not well known. The observations through molecular lines, in nearby clouds with millimetric interferometry, detect structures down to 0.01pc currently, and even in high-latitude clouds distant by 100 pc, structures down to 400 AU ($2 \cdot 10^{-3}$ pc). Through VLBI, it is possible to go much further. HI is detected and mapped in absorption in front of remote quasars (Diamond et al 1989, Davis et al 1996), and contrasted structures of 20 AU are ubiquitous. This small-scale structure is also traced by the interstellar scattering, and in particular extreme scattering events or ESE (Fiedler et al 1987, 1994). The statistics on ESE is so large that we know approximately the number of small clumps in the Galaxy: they are about 1000 times more numerous than stars. If these objects are self-gravitating, at the end of the ISM hierarchy, their mass is of the order of $10^{-3} M_{\odot}$, and they represent a significant mass component of the Galaxy (Pfenniger & Combes 1994).

Self-gravity is widely accepted as dominant process in the ISM. Gravitational collapse is accompanied by fragmentation in a system with very efficient cooling, and this process can provide the turbulent motions observed. The theory was first proposed by Hoyle (1953) who showed that the isothermal collapse of a cloud led to recursive fragmentation, since the Jeans length decreases faster than the cloud radius. Rees (1976) has determined the size of the smallest fragments, when they become opaque to their own radiation. They correspond roughly to the smallest scales observed in the ISM (sizes of 10 AU, and masses of $10^{-3} M_{\odot}$, see the physical parameters of the "clumpuscles" in Pfenniger & Combes 1994). Many other physical processes play a role in the turbulent ISM, as for instance rotation and magnetic fields. But they cannot be identified as the motor and the origin of the structure. Galactic rotation certainly injects energy at the largest scales, but angular momentum cannot cascade down the hierarchy of clouds; indeed if the rotational velocity is too high, the structure is unstable to clump formation (cf Toomre criterium, 1964), and the non-axisymmetry evacuates angular momentum outside the structure. Magnetic fields are certainly enhanced by the turbulent motions, and could reach a certain degree of global equipartition with gravitational and kinetic energies

in the virialised clouds. But they cannot be alone at the origin of the hierarchical structure, gravity has to trigger the collapse first. Besides, there is no observational evidence of the gas collapse along the field lines, polarisation measurements give contradictory results for the field orientation with respect to the gas filaments. Therefore, although rotation, turbulence, magnetic fields play an important role in the ISM, they are more likely to be consequences of the formation of the structure.

2.7. SIMULATIONS

A large number of hydrodynamical simulations have been run, in order to reproduce the hierarchical density structure of the interstellar medium. However, these are not yet conclusive, since the dynamical range available is still restricted, due to huge computational requirements.

It has been argued that self-similar statistics alone can generate the observed structure of the ISM, in pressureless turbulent flows without self-gravity (Vazquez-Semadeni 1994); however, only three levels of hierarchical nesting can be traced.

From the size-linewidth relation $\sigma \propto R^{1/2}$, and the second observed scaling law $\rho \propto R^{-1}$, it can be deduced that

$$\sigma \propto \rho^{-1/2}$$

and therefore, if the turbulent pressure P is defined as usual by

$$dP/d\rho = \sigma^2$$

it follows that

$$P \propto \log \rho$$

which is the logatropic equation of state, or "logatropé". This behaviour has been tested in simulations (e.g. Vazquez-Semadeni et al 1998), but the logatropé has not been found adequate to represent dynamical processes occurring in the ISM (either hydro, or magnetic 2D simulations). The equation of state of the gas would be more similar to a polytrope of index $\gamma \approx 2$. But the results could depend whether the clouds are in approximate equilibrium or not (cf McLaughlin & Pudritz 1996).

Vazquez-Semadeni et al (1997) have searched for Larson relations in the results of 2D self-gravitating hydro (and MHD) simulations of turbulent ISM: they do not find clear relations, but instead a large range of sizes at a given density, and a large range of column densities; they suggest that the observational results could be artefacts or selection

effects (existence of a threshold in column density for UV-shielding for example).

3. Galaxy Distributions

It has long been recognized that galaxies are not distributed homogeneously in the sky, but they follow a hierarchical structure: galaxies gather in groups, that are embedded in clusters, then in superclusters, and so on (Shapley 1934, Abell 1958). Moreover, galaxies and clusters appear to obey scaling properties, such as the power-law of the two point-correlation function:

$$\xi(r) \propto r^{-\gamma}$$

with the slope γ , the same for galaxies and clusters, of ≈ 1.7 (e.g. Peebles, 1980, 1993).

3.1. CORRELATION FUNCTIONS

The correlation function is defined as

$$\xi(r) = \frac{\langle n(r_i).n(r_i+r) \rangle}{\langle n \rangle^2} - 1$$

where $n(r)$ is the number density of galaxies, and $\langle \dots \rangle$ is the volume average (over d^3r_i). One can always define a correlation length r_0 by $\xi(r_0) = 1$.

This definition involves the average density $\langle n \rangle$, which depends on the scale for the galaxy distribution, since it is a fractal, at least over a certain range of scales. There has been considerable debate about this (see Davis 1997, Pietronero et al 1997). If everybody agrees that the universe is a fractal below 200 Mpc scales, the question is not settled as of the scale beyond which the universe is homogeneous. Pietronero et al (1997) claim that this limiting scale has not yet been reached in the present catalogs, since large-scale structures are still found at any scale. On the contrary, Davis & Peebles (1983) or Hamilton (1993) argue that the galaxy-galaxy correlation length r_0 is rather small. The most frequently reported value is $r_0 \approx 5h^{-1}$ Mpc (where $h = H_0/100\text{km s}^{-1}\text{Mpc}^{-1}$).

The problem is that the definition of $\xi(r)$ includes a normalisation by the average density of the universe, which, if the homogeneity scale is not reached, depends on the size of the galaxy sample.¹

This implies a correlation length that should increase with the distance limits of galaxy catalogs, as it indeed does (Davis et al 1988). The same problem occurs for the two-point correlation function of galaxy clusters; the corresponding $\xi(r)$ has the same power law as galaxies, their length r_0 has been reported to be about $r_0 \approx 25h^{-1}$ Mpc, and their correlation amplitude is therefore about 15 times higher than that of galaxies (Postman, Geller & Huchra 1986, Postman, Huchra & Geller 1992). The latter is difficult to understand, unless there is a considerable difference between galaxies belonging to clusters and field galaxies (or morphological segregation). The other obvious explanation is that the normalizing average density of the universe was then chosen lower.

Assuming that the average density is a constant, while homogeneity is not yet reached, could perturb significantly the correlation function, and its slope, as shown by Coleman, Pietronero & Sanders (1988) and Coleman & Pietronero (1992). The function $\xi(r)$ has a power-law behaviour of slope $-\gamma$ for $r < r_0$, then it turns down to zero rather quickly at the statistical limit of the sample. This rapid fall leads to an over-estimate of the small-scale γ . Pietronero (1987) introduces the conditional density

$$\Gamma(r) = \frac{\langle n(r_i).n(r_i + r) \rangle}{\langle n \rangle}$$

which is the average density around an occupied point. For a fractal medium, where the mass depends on the size as

$$M(r) \propto r^D$$

D being the fractal (Hausdorff) dimension, the conditional density behaves as

$$\Gamma(r) \propto r^{D-3}$$

It is possible to retrieve the correlation function as

$$\xi(r) = \frac{\Gamma(r)}{\langle n \rangle} - 1$$

In the general use of $\xi(r)$, $\langle n \rangle$ is taken for a constant, and we can see that

$$D = 3 - \gamma \quad .$$

¹ The notion of correlation length ξ_0 is usually different in physics, where ξ_0 characterizes the exponential decay of correlations ($\sim e^{-r/\xi_0}$). For power decaying correlations, it is said that the correlation length is infinite

If for very small scales, both $\xi(r)$ and $\Gamma(r)$ have the same power-law behaviour, with the same slope $-\gamma$, then the slope appears to steepen for $\xi(r)$ when approaching the length r_0 . This explains why with a correct statistical analysis (Di Nella et al 1996, Sylos Labini & Amendola 1996, Sylos Labini et al 1996), the actual $\gamma \approx 1 - 1.5$ is smaller than that obtained using $\xi(r)$ (cf 2). This also explains why the amplitude of $\xi(r)$ and r_0 increases with the sample size, and for clusters as well.

3.2. HOMOGENEITY HYPOTHESIS AND COSMOLOGICAL PRINCIPLE

Isotropy and homogeneity are expected at very large scales from the Cosmological Principle (e.g. Peebles 1993). However, this does not imply local or mid-scale homogeneity (e.g. Mandelbrot 1982, Sylos Labini 1994): a fractal structure can be locally isotropic, but inhomogeneous. The main observational evidence in favor of the Cosmological Principle is the remarkable isotropy of the cosmic background radiation (e.g. Smoot et al 1992), that provides information about the Universe at the matter/radiation decoupling. There must therefore exist a transition between the small-scale fractality to large-scale homogeneity. This transition is certainly smooth, and might correspond to the transition from linear perturbations to the non-linear gravitational collapse of structures. The present catalogs do not yet see the transition since they do not look up sufficiently back in time. It can be noticed that some recent surveys begin to see a different power-law behavior at large scales ($\lambda \approx 200 - 400h^{-1}$ Mpc, e.g. Lin et al 1996).

3.3. THE PROBLEM AND METHODS

It is generally recognized that the galaxy structures in the Universe have developed by gravitational collapse from primordial fluctuations. Once unstable, density fluctuations do not grow as fast as we are used to for Jeans instability (exponential), since they are slowed down by expansion. The rate of growth is instead a power-law. Let us call the density contrast δ :

$$\delta(\vec{x}) = (\rho(\vec{x}) - \langle \rho \rangle) / \langle \rho \rangle$$

where $\langle \rho \rangle$ is the mean density of the Universe, assumed homogeneous at very large scale. If \vec{r} is the physical coordinate, the comoving coordinate \vec{x} is defined by:

$$\vec{r} = a(t)\vec{x}$$

where $a(t)$ is the scale factor, accounting for the Hubble expansion (normalised to $a(t_0) = 1$ at the present time). Since the Hubble constant verifies $H(t) = \dot{a}/a$, the peculiar velocity is defined by

$$\vec{v} = \dot{\vec{r}} - H\vec{r} = a\dot{\vec{x}}$$

In comoving coordinates, the Poisson equation becomes:

$$\nabla_x^2 \Phi = 4\pi G a^2 (\rho - \langle \rho \rangle)$$

It can be shown easily that in a flat universe, the density contrast in the linear regime grows as the scale factor $a(t) = (t/t_0)^{2/3}$ (this is also approximately true for any universe in the early times). An exact solution for the non-linear collapses exist only in very special conditions, such as the spherical collapse. For the well-known top-hat perturbation, an overdensity reaches the singularity in a finite collapse time t_c , when its corresponding linear density contrast would have reached the value

$$\delta_c \approx 1.69$$

The evolution of its radius follows the Friedman solution for a density above critical; it reaches a maximum radius, before virializing to a radius equal to half that one. Its final density contrast is 178 (both figures, although indicative, are widely used in the domain).

The level of fluctuations was very small (about 10^{-5} at the scale of COBE resolution, i.e. 7°) at the last scattering surface, just before matter recombination, about 10^5 yr after the Big-Bang. At first, the development of the structures is easy to compute, since they are in the linear regime, and interactions between scales can be neglected (cf Peebles 1980). Then, in the non-linear regime, no analytical solution exists, and one should resort to approximations, or full N-body simulations.

3.3.1. Numerical simulations

N-body computations have been widely used, to gravitationally follow the non-linear evolution of the fluctuations. From a comparison of the results with today galaxy distribution, one can hope to trace back the initial mass spectrum of fluctuations, and to test postulated cosmologies such as CDM and related variants (cf Ostriker 1993). However, the evolution depends on many free parameters, the gas physics, the star formation feedback, the amount and physics of dark matter. This approach has not yet yielded definite results, also because numerical limitations (restricted dynamical range due to the softening and limited volume) have often masked the expected self-similar behavior (Colombi et al 1996).

3.3.2. *Zel'dovich approximation*

The first approximation has been pioneered by Zel'dovich (1970): it consists to assume that the pressure forces are negligible in the first collapsing structures, since they are much bigger than the Jeans length. This is particularly adapted to the top-down scenario of adiabatic fluctuations, where photons and baryons both fluctuate, such that entropy is conserved. In that case, the matter-photon coupling will prevent the development of large amplitudes fluctuations at small-scales. Large-scales are then the first to collapse, and they fragment in smaller structures. In this approximation, the particles maintain their peculiar velocities in comoving space, and collapse in 1D filaments, or 2D sheets or pancakes (cf formation of caustics). After collapse, the approximation fails since particles diffuse away; an artificial viscosity has then been introduced, so that particles cannot cross each other, and the pancakes remain coherent, it is the "adhesion model" (Shandarin & Zel'dovich 1989). The velocity field is governed by a Burgers equation, for which analytical solutions are known (Vergassola et al 1994).

Related to this approach is the Lagrangian approximation, which in fact pushes the Zel'dovich approximation to further orders. Since this approach fails as soon as orbits are crossing (i.e. multi-streaming) it is assumed that this multi-streaming at small scales has negligible consequences at large-scales (Lachièze-Rey 1993).

The success of this approximation has been boosted by the fact that the self-gravitating Universe appears filamentary. The reason for this is probably that many collapsing structures are larger than the Jeans mass; also in realistic scenarios, the collapse is not spherical, but does form sheets and filaments (Larson 1985). The latter have the advantage that in 1D, pressure forces have always the same dependence with radius than the gravity forces, and therefore cannot halt the collapse, whatever the cooling (Uehara et al. 1996; Inutsuka & Miyama 1997).

3.3.3. *BBGKY hierarchy*

A second approach, which should work essentially in the linear (or weakly non-linear) regime, is to solve the BBGKY hierarchy of equations, a method which has been successfully used in plasma physics. However, the hierarchy is here infinite, and approximations should be made for closure (Davis & Peebles 1977; Balian & Schaeffer 1989). The main assumption is that the N -points correlation functions are scale-invariant and behave as power-laws like is observed for the few-body correlation functions. Crucial to this approach is the determination of the void probability, which is a series expansion of the N -points correlation functions (White 1979). The hierarchical solutions found in this

frame agree well with the simulations, and with the fractal structure of the universe at small-scales (Balian & Schaeffer 1988).

3.3.4. *Thermodynamical approach*

A third approach is the thermodynamics of gravitating systems, developed by Saslaw & Hamilton (1984), which assumes quasi thermodynamic equilibrium. The latter is justified at the small-scales of non-linear clustering, since the expansion time-scale is slow with respect to local relaxation times. Indeed the main effect of expansion is to subtract the mean gravitational field, which is negligible for structures of mean densities several orders of magnitude above average. The predictions of the thermodynamical theory have been successfully compared with N-body simulations (Itoh et al 1993), but a special physical parameter (the ratio of gravitational correlation energy to thermal energy) had to be adjusted for a better fit (Bouchet et al 1991, Sheth & Saslaw 1996, Saslaw & Fang 1996).

3.4. MASS FUNCTION, PRESS-SCHECHTER FORMALISM

In 1974, Press and Schechter developed a formalism to predict the mass function of galaxies and structures in the Universe, assuming that gravitational collapse in an expanding universe non-linearly evolves through a self-similar spectrum (PS74). The resulting mass function is independent of the initial spectrum of condensations assumed. The non-linear N-body interactions randomize the initial positions and generate perturbations to all other scales: the growth of large scale condensations from non-linear clumping of smaller ones occurring much faster than their linear growth, a self-similar universal spectrum is established, only from seeds corresponding to the Jeans mass at recombination ($\approx 10^7 M_{\odot}$).

This led to an excellent fit of the galaxy luminosity function proposed by Schechter (1976):

$$\Phi(L) \propto L^{-\alpha} \exp(-L/L_*)$$

where L_* is a characteristic galaxy luminosity, and $\alpha \sim 1$.

In order to derive the mass function, i.e. the number density of structures of mass between M and $M+dM$, $n(M)$, PS74 first assume that a structure collapses as soon as the extrapolated linear density contrast δ_c is of the order of 1. Since in the spherical top-hat case (see section 3.3) the collapse occurs in a time-scale corresponding to a linear $\delta_c = 1.69$, this indicative value of δ_c is taken. The fraction of collapsed mass, at any resolution smaller than R is:

$$F(< R) = \int_{\delta_c}^{\infty} P(\delta, R) d\delta$$

For gaussian random phase fluctuations, the probability $P(\delta, R)$ is

$$P(\delta, R) = (2\pi)^{-1/2} / \delta_* \exp(-\delta^2 / (2\delta_*^2))$$

where δ_* is the standard deviation, obtained at scale R

$$\delta_* = (\langle M^2 \rangle - \langle M \rangle^2)^{1/2} / M$$

Then the fraction $F(< R)$ becomes:

$$F(< R) = 1/2 \operatorname{erfc}(2^{-1/2} \delta_c / \delta_*)$$

where erfc is the complementary error function.

To relate this to the mass associate to the scale R , we use $M = 4\pi < \rho > R^3 / 3$, justified for the top-hat smoothing function (to obtain the average ρ). The function $F(< R)$ gives the probability for a scale R to be bound, but it could also be part of another larger bound scale, so the fraction of independent masses, with mass between M and $M + dM$, that have collapsed is the derivative of it with respect to mass M :

$$dF/dM = 1/2 (2\pi)^{-1/2} \delta_c / \delta_* M^{-1} \exp(-\frac{1}{2} \frac{\delta_c^2}{\delta_*^2})$$

The mass density due to condensations of mass M is then obtained by multiplying by the total number density at the same epoch ρ/M . However, PS74 realised that the integral of the fraction F was 1/2 instead of 1, i.e. that the formula accounted for only one half of the mass in the universe. They multiplied by a factor 2 to include the underdense regions that would accrete on the collapsed objects. This is a typical problem of the linear theory, where only half of the mass is in overdense regions. Also called the cloud-in-cloud problem, this factor 2 puzzle has been better explained later (Cole 1989, Bond et al 1991, White & Kauffman 1994).

This formalism has been recently widely used, since it gives excellent agreement with N-body simulations, and provides a way to compute easily the merging histories of galaxies (Lacey & Cole 1993, 1994).

If we make the particular assumption that the power spectrum of the fluctuations $P(k)$ (i.e. the square of the module of δ_k the Fourier transform of δ) is $P(k) \propto k^n$, then $\delta_* \propto M^{-(n+3)/6}$, and the PS formula becomes

$$n(M) dM = \langle \rho \rangle / M_*^2 / \operatorname{sqr}(2\pi) (n+3) / 6 (M/M_*)^{(n+3)/6-2}$$

$$\exp(-1/2(M/M_*)^{(n+3)/3})dM$$

where M_* is the mass corresponding to the scale at which the amplitude δ_* reaches δ_c .

3.5. MULTIFRACTALS

The idea of fractals as a good representation of the self-similar clustering hierarchy of galaxies has been proposed very early (de Vaucouleurs 1960, 1970; Mandelbrot 1975). Since then, many authors have shown that a fractal distribution indeed reproduces quite well the aspect of galaxy catalogs, for example by simulating a fractal and observing it, as with a telescope (Scott, Shane & Swanson, 1954; Soneira & Peebles 1978). When going into details, however, the distribution of galaxies might appear more complex: first of all, catalogs are weighted by the luminosity distribution, and not the mass distribution, and these are not equivalent. For instance, there is a luminosity segregation in clusters of galaxies, and slightly different fractal dimensions can be obtained with different galaxy-types (elliptical/spirals/dwarfs). Also determination of masses of structures through different ways (X-rays, gravitational lensing, etc..) suggest that the dark matter is not exactly distributed as light, and there could be a significant bias. All this has led to the introduction of multifractality to represent the Universe (e.g. Sylos-Labini & Pietronero 1996). In a multifractal system, local scaling properties slightly evolve, and can be defined by a continuous distribution of exponents. This is a mere generalisation of a simple fractal, that links the space and mass distributions. Multifractality may also better account for the transition to homogeneity, with a fractal dimension varying with scale (Balian & Schaeffer 1989, Castagnoli & Provenzale 1991, Martinez et al 1993, Dubrulle & Lachièze-Rey 1994).

4. Bases for a Statistical Field theory

Both for the ISM and for galaxy distributions in the Universe, self-similar structures are observed over large ranges in scales. Scaling laws are observed, which translate by an average density decreasing with scale as a power-law, of slope $-\gamma$ between -1.5 and -1, corresponding to a fractal dimension $D = 3 - \gamma$ between 1.5 and 2.

We propose in the following that self-gravity is a dominant factor in the two media, and try to establish a statistical theory in the hope to explain the fractal structure. The theory should not only account

for the existence of the structure, but also be able to predict its fractal dimension and others critical exponents (de Vega, Sanchez & Combes, 1996a,b, 1998).

Since gravity is scale-independent, there are opportunities for a mechanism to propagate over scales in a self-similar fashion. For the ISM, in a quasi isothermal regime, a fractal structure could be build through recursive Jeans instability and fragmentation. This recursive fragmentation proceeds until the density is high enough to reach the adiabatic regime. Self-gravity could be the principal origin of the fractal, with generated turbulent motions in virial equilibrium at each scale. For galaxy formation, the smallest structures collapse first, and these influence the largest scale in a non-linear manner. It is obvious that in both cases, the system does not tend to a stationary point, but develops fluctuations at all scales, and these must be studied statistically.

In order to study its thermodynamics properties, we develop the grand partition function of the ensemble of self-gravitating particles (section 4.1). In transforming the partition function through a functional integral (section 4.2), it can be shown that the system is exactly equivalent to a scalar field theory (section 4.3). The theory does not diverge, since the system is considered only between two scale limits: the short-scale and large-scale cut-offs. Through a perturbative approach it can be demonstrated that the system has a critical behaviour, for any parameter (effective temperature and density). That is, we can consider the self-gravitating gaseous medium as correlated at any scale, as for the critical points phenomena in phase transitions (as was first suggested by Totsuji & Kihara 1969).

Since scaling behaviours are the best studied through renormalization group theory, we use these methods to derive by analogy the critical exponents of the system (section 5). The aim, that will be developped more fully in the following, is to relate the critical exponents of well known universal critical phenomena, to the Hausdorff dimension of the astrophysics fractals.

4.1. HAMILTONIAN OF THE SELF-GRAVITATING ENSEMBLE OF N-BODIES

Let us consider a gas of particles submitted only to their self-gravity, in thermal equilibrium at temperature T ($kT = \beta^{-1}$). In the interstellar medium, quasi isothermality is justified, due to the very efficient cooling. For unperturbed gas in the outer parts of galaxies, gas is in equilibrium with the cosmic background radiation at $T \approx 3K$ (Pfenninger et al 1994, Pfenninger & Combes 1994). For a system of collapsing

structures in the universe, this can be a valid approximation, as soon as the gradient of temperature is small over a given scale.

This isothermal character is essential for the description of the gravitational systems as critical systems, as will be shown later, so that the canonical ensemble appears the best adapted system. We do not consider isolated gravitational systems, for which the microcanonical system is generally used (e.g. Horwitz & Katz 1978a,b; Padmanabhan 1990). However, for easy mathematical development, we develop the partition function in the grand canonical ensemble, allowing for a variable number of particles N (for application to real systems, constant masses will later be considered). The grand partition function \mathcal{Z} and the Hamiltonian H_N are

$$\mathcal{Z} = \sum_{N=0}^{\infty} \frac{z^N}{N!} \int \cdots \int \prod_{l=1}^N \frac{d^3 p_l d^3 q_l}{h^3} e^{-\beta H_N}$$

$$H_N = \sum_{l=1}^N \frac{p_l^2}{2m} - G m^2 \sum_{1 \leq l < j \leq N} \frac{1}{|\vec{q}_l - \vec{q}_j|}$$

where z is the fugacity = $\exp(-\beta\mu_c)$ in terms of the gravito-chemical potential μ_c .

This can be transformed, with continuous density $\rho(\vec{r}) = \sum_{j=1}^N \delta(\vec{r} - \vec{q}_j)$

$$\frac{1}{2} \beta G m^2 \sum_{1 \leq l \neq j \leq N} \frac{1}{|\vec{q}_l - \vec{q}_j|} = \frac{1}{2} \beta G m^2 \int_{|\vec{x} - \vec{y}| > a} \frac{d^3 x d^3 y}{|\vec{x} - \vec{y}|} \rho(\vec{x}) \rho(\vec{y})$$

The cutoff a is here introduced naturally, it corresponds to the size of the smallest fragments, or clumpscules (of the order of ~ 10 AU). In fact, we consider that the particles of the system interact with the Newton law of gravity ($1/r$) only within the size range of the fractal, where self-gravity is predominant. At small scale, other forces enter into account, and we can adopt a model of hard spheres to schematize them. Also at large scales, beyond the upper cutoff, different forces must be introduced. The phenomenological potential thus considered does not possess any singularity.

4.2. GRAND PARTITION FUNCTION AS A FUNCTIONAL

Using the potential in $1/r$, and its inverse operator $-\frac{1}{4\pi} \nabla^2$ (but see also a similar derivation, with $[1 - \theta(a - r)]/r$ and its corresponding inverse

operator, for the phenomenological potential with cutoff, in de Vega et al 1996b), the exponent of the potential energy can be represented as a functional integral (Stratonovich 1958, Hubbard 1959)

$$\begin{aligned}
e^{\frac{1}{2}\beta G m^2 \int \frac{d^3x d^3y}{|\vec{x}-\vec{y}|} \rho(\vec{x})\rho(\vec{y})} &= \int \int \mathcal{D}\xi e^{-\frac{1}{2} \int d^3x (\nabla\xi)^2 + 2m\sqrt{\pi G\beta} \int d^3x \xi(\vec{x}) \rho(\vec{x})} \\
\mathcal{Z} &= \sum_{N=0}^{\infty} \frac{1}{N!} \left[z \left(\frac{2\pi m}{h^2\beta} \right)^{3/2} \right]^N \int \int \mathcal{D}\xi e^{-\frac{1}{2} \int d^3x (\nabla\xi)^2} \int \dots \int \prod_{l=1}^N d^3q_l e^{2m\sqrt{\pi G\beta} \sum_{l=1}^N \xi(\vec{q}_l)} \\
&= \int \int \mathcal{D}\xi e^{-\frac{1}{2} \int d^3x (\nabla\xi)^2} \sum_{N=0}^{\infty} \frac{1}{N!} \left[z \left(\frac{2\pi m}{h^2\beta} \right)^{3/2} \right]^N \left[\int d^3q e^{2m\sqrt{\pi G\beta} \xi(\vec{q})} \right]^N \\
&= \int \int \mathcal{D}\xi e^{-\int d^3x \left[\frac{1}{2}(\nabla\xi)^2 - z \left(\frac{m}{2\pi\beta} \right)^{3/2} e^{2m\sqrt{\pi G\beta} \xi(\vec{x})} \right]}
\end{aligned}$$

With the following change of variables:

$$\phi(\vec{x}) \equiv 2m\sqrt{\pi G\beta} \xi(\vec{x})$$

$$\mathcal{Z} = \int \int \mathcal{D}\phi e^{-\frac{1}{T_{eff}} \int d^3x \left[\frac{1}{2}(\nabla\phi)^2 - \mu^2 e^{\phi(\vec{x})} \right]}$$

where

$$\mu^2 = \frac{\pi^{5/2}}{h^3} z G (2m)^{7/2} \sqrt{kT} \quad , \quad T_{eff} = 4\pi \frac{G m^2}{kT}$$

(note that the "equivalent" temperature in the field theory is in fact inversely proportional to the physical temperature). It can be shown that the parameter μ is equal to the inverse of the Jeans length, itself of the order of the cutoff a .

4.3. INTRODUCTION OF A LOCAL SCALAR FIELD, WITH EXPONENTIAL SELF-INTERACTION

The main point of the previous derivation is that the partition function for the gas of particles in gravitational interaction has been transformed into the partition function for a single scalar field $\phi(\vec{x})$ with local action

$$S[\phi(\cdot)] \equiv \frac{1}{T_{eff}} \int d^3x \left[\frac{1}{2}(\nabla\phi)^2 - \mu^2 e^{\phi(\vec{x})} \right]$$

Apparently, the term $-\mu^2 e^{\phi(\vec{x})}$ makes the ϕ -field energy density diverge, which is related to the attractive character of the gravitational force. But the physical short-distance cutoff a eliminates the zero distance singularity. It is then possible to compute the statistical average value of the density $\rho(\vec{r})$

$$\langle \rho(\vec{r}) \rangle = \mathcal{Z}^{-1} \sum_{N=0}^{\infty} \frac{1}{N!} \left[z \left(\frac{m}{2\pi\beta} \right)^{3/2} \right]^N \int \int \prod_{l=1}^N d^3 q_l \rho(\vec{r}) e^{\frac{1}{2}\beta G m^2 \sum_{1 \leq l \neq j \leq N} \frac{1}{|\vec{q}_l - \vec{q}_j|}}$$

Or in the ϕ -field language, the particle density expresses as

$$\langle \rho(\vec{r}) \rangle = -\frac{1}{T_{eff}} \langle \nabla^2 \phi(\vec{r}) \rangle = \frac{\mu^2}{T_{eff}} \langle e^{\phi(\vec{r})} \rangle$$

where $\langle \dots \rangle$ means functional average over $\phi(\cdot)$ with statistical weight $e^{S[\phi(\cdot)]}$. Density correlators are

$$C(\vec{r}_1, \vec{r}_2) \equiv \langle \rho(\vec{r}_1) \rho(\vec{r}_2) \rangle - \langle \rho(\vec{r}_1) \rangle \langle \rho(\vec{r}_2) \rangle$$

$$C(\vec{r}_1, \vec{r}_2) = \frac{\mu^4}{T_{eff}^2} \left[\langle e^{\phi(\vec{r}_1)} e^{\phi(\vec{r}_2)} \rangle - \langle e^{\phi(\vec{r}_1)} \rangle \langle e^{\phi(\vec{r}_2)} \rangle \right]$$

4.4. STATIONARY POINTS AND HYDROSTATIC SOLUTIONS

The equation for stationary points:

$$\nabla^2 \phi = -\mu^2 e^{\phi(\vec{x})}$$

can be expressed in terms of the gravitational potential $U(\vec{x})$

$$\nabla^2 U(\vec{r}) = 4\pi G z m \left(\frac{2\pi m k T}{h^2} \right)^{3/2} e^{-\frac{m}{kT} U(\vec{r})}$$

This corresponds to the Poisson equation for an ideal gas in hydrostatic equilibrium:

$$\nabla P(\vec{r}) = -m \rho(\vec{r}) \nabla U(\vec{r})$$

where $P(\vec{r})$ stands for the pressure. Combined with the equation of state for the ideal gas

$$P = kT \rho$$

this yields for the particle density

$$\rho(\vec{r}) = \rho_0 e^{-\frac{m}{kT} U(\vec{r})}$$

where ρ_0 is a constant.

The ϕ -field has special properties under scale transformations

$$\vec{x} \rightarrow \vec{x}_\lambda \equiv \lambda \vec{x}$$

where λ is an arbitrary real number. For any solution $\phi(\vec{x})$ of the stationary point equations, there is a family of dilated solutions of the same equation

$$\phi_\lambda(\vec{x}) \equiv \phi(\lambda \vec{x}) + \log \lambda^2$$

In addition, $S[\phi_\lambda(\cdot)] = \lambda^{-1} S[\phi(\cdot)]$. A rotationally invariant stationary point is given by

$$\phi^c(r) = \log \frac{2}{\mu^2 r^2}$$

This singular solution, where can be recognized the isothermal sphere, is invariant under the scale transformations, i.e.

$$\phi_\lambda^c(r) = \phi^c(r)$$

The only constant stationary solution is the singular $\phi_0 = -\infty$.

With a perturbative method, starting from the stationary solution $\phi_0 = -\infty$, it can be obtained for large distances (de Vega et al 1996b)

$$C(\vec{r}_1, \vec{r}_2) \stackrel{|\vec{r}_1 - \vec{r}_2| \rightarrow \infty}{\approx} \frac{\mu^4}{2 C_D^2 |\vec{r}_1 - \vec{r}_2|^2} + O(|\vec{r}_1 - \vec{r}_2|^{-3})$$

showing that the ϕ -field theory scales, and behaves critically for a continuum set of values of μ and T_{eff} .

5. Renormalization Group Methods

The renormalization methods are very powerful to deal with self-similar systems obeying scaling laws, like critical phenomena. In the latter case, exemplified by second order phase transitions, there exist critical divergences, where physical quantities become singular as power-laws of parameters called critical exponents. These critical systems reveal a collective behaviour, organized from microscopic degrees of freedom, through giant fluctuations and statistical correlations. Hierarchical structures are built up, coupling all scales together, replacing an homogeneous system in a scale-invariant system. It can be shown that local forces are not important to describe the collective behaviour, which is only due to the statistical coupling of local interactions. Therefore, critical exponents depend only on the statistical distribution of

microscopic configurations, i.e. on the dimensionalities or symmetries of the system. There exist wide universality classes, that allow to draw quantitative predictions on the system from only a qualitative knowledge of its properties (e.g. Parisi, 1988; Zinn-Justin 1989; Binney et al 1992).

5.1. CRITICAL PHENOMENA

Critical phenomena occur at second order phase transitions, i.e. continuous transitions without latent heat. The paradigm of these systems is the transition at the Curie point ($T=T_c= 1043\text{K}$) from paramagnetic iron, where the magnetic moment is proportional to the applied field $m=\mu B$, to ferromagnetic state, where there exists a permanent magnetic moment m_0 even in zero field. Another well known example is the critical point of water, at which the transition from the liquid to gas becomes continuous (at $T_c = 647 \text{ K}$, $\rho_c = 0.323 \text{ g cm}^{-3}$).

Although the permanent magnet tends to zero continuously at T_c , there are divergences: for instance the heat capacity C behaves as $C \propto |T - T_c|^{-\alpha}$, with $\alpha > 0$. Also the magnetic susceptibility

$$\chi_T = \partial m / \partial B_T \propto |T - T_c|^{-\gamma}$$

(or for the case of H_2O , the compressibility $\kappa_T \propto |T - T_c|^{-\gamma}$).

At the critical point, it is easy to understand that the compressibility which tends to infinity generates large density fluctuations, and therefore light is strongly diffused by the varying optical index: this is the critical opalescence. The extraordinary fact is that microscopic forces can give rise to large-scale fluctuations, as if the medium was organized at all scales.

5.1.1. Order parameter and correlation function

The order parameter is defined by the characteristic physical quantity which experiences large fluctuations at criticality. For the H_2O case, it is a scalar field

$$\Phi(x) = \rho(x) - \rho_{gas}(x)$$

for a spin system, it is a vector field ($\sum s_i$), according to the dimensionality adopted. The critical point is particularly well characterized through the correlation functions. The two-point correlation function is

$$G^{(2)}(r) = \langle \Phi(0) \cdot \Phi(r) \rangle$$

where brackets mean statistical (thermal) average, over all configurations, and the connected correlation function is

$$G_c^{(2)}(r) = \langle \Phi(0) \cdot \Phi(r) \rangle - | \langle \Phi \rangle |^2$$

which is independent of the mean value. At critical point, for large distances r

$$G_c^{(2)}(r) \propto r^{2-d-\eta}$$

where d is the space dimension, and η a critical exponent. Far from the critical point,

$$G_c^{(2)}(r) \propto \exp(-r/\xi)$$

where $\xi \propto |T - T_c|^{-\nu}$ is the correlation length, and ν another critical exponent.

5.1.2. *Universality, Dimensionality, Symmetry*

Experiments have shown that the critical exponents for a wide variety of systems are the same, and more precisely they belong to universality classes, depending only on the dimensionality d of space and D of the order parameter (for instance if the field is scalar or a vector with dimension D). This universality means that the details of the local forces are unimportant; therefore the local interactions can be simply modelled, through a schematic hamiltonian supposed to hold the relevant symmetries of the system.

Generally, the thermodynamic functions, such as the free energy F (from which the heat capacity $C = -T\partial^2 F/\partial T^2$ can be derived) can be decomposed in a regular part, and a singular part. The latter contain non-integer exponents (such as some derivatives diverge) as a function of $|T - T_c|$. Only the singular part with its critical exponents are universal, but the regular part could be dominant for some functions.

The 6 critical exponents, α , β , γ , δ , ν and η are in fact not independent. From the Widom & Kadanoff scaling hypotheses, four relations can be derived between them. These relations can be demonstrated rigorously through renormalization theory. They are:

$$2\beta + \gamma = 2 - \alpha = 2\beta\delta - \gamma$$

$$\gamma = \nu(2 - \eta)$$

$$\nu d = 2 - \alpha$$

where d is the space dimension of the problem. There exists therefore only 2 independent critical exponents.

5.2. THE ISING MODEL

The essential physical phenomena occurring when a system undergoes a continuous phase transition are reproduced in simplified models, that have played the role of prototypes. They consider a field (order parameter) defined on a lattice of N sites, of dimension d . For the Ising model

of ferromagnets, the field is the spin value at each site, i.e. s_i . We will consider only two possible values for s_i , +1 or -1, so that the order parameter is a scalar ($D = 1$).

The Ising model was resolved for $d = 1$ by Ising in 1925, for $d = 2$ by Onsager in 1944, and with B non zero only recently (Zamalodchikov 1989). There is not yet any analytical solution for $d = 3$.

The Hamiltonian of the system can be written:

$$H = 1/2 \sum_{ij} J_{ij} s_i s_j - B \sum_i s_i$$

where B is the external magnetic field, and the interaction constant

$$J_{ij} = J$$

if i and j are neighbouring sites, and 0 otherwise. For ferromagnets, $J < 0$ and spins tend to align parallel to one another, while $J > 0$ will correspond to anti-ferromagnets.

The partition function of the system in zero B can be written as:

$$Z = \sum_{s_i} \exp(-\beta H) = \sum_{s_i} \exp(-0.5\beta \sum_{ij} J_{ij} s_i s_j)$$

Any physical quantity can then be derived, by summing over the possible configurations α , such as the average energy:

$$U = \langle E \rangle = 1/Z \sum_{\alpha} E_{\alpha} \exp(-\beta E_{\alpha}) = -\partial \log Z / \partial \beta_V$$

and the heat capacity in particular:

$$\langle E^2 \rangle - \langle E \rangle^2 = \partial^2 \log Z / \partial \beta_V^2 = C_V / k \beta^2$$

In the same way, correlation functions are expressed as second derivatives of the partition function. Since these summations are in general intractable analytically, one has recourse to numerical techniques.

5.3. MONTE-CARLO NUMERICAL CALCULATIONS

The principle is to calculate directly the statistical averages

$$\langle X \rangle = 1/Z \sum_{\alpha} X_{\alpha} \exp(-\beta E_{\alpha})$$

But the number of terms to compute grows exponentially with the size of the system; let us consider for example the Ising model in $d =$

2, on a small lattice 3x3, the number of configurations is $2^9 = 512$, which induces reasonable computations. But for a simple lattice 10x10, there are already $2^{100} \approx 1.3 \cdot 10^{30}$ configurations; even with a sustained computational speed of 1 GFlop, this will require more than $3 \cdot 10^{13}$ yr, i.e. more than a thousand Hubble times. Clearly, the method is to consider judicious samples of the ensemble of configurations. There are configurations that are much less probable, and they will contribute negligibly.

The most simple method is the Metropolis one; it computes the statistical averages in a certain number of steps (typically 10^6 steps or more), each step corresponding to a configuration of the system. Initially, the system is placed in a simple state (for instance all spins aligned), but far from equilibrium. A certain number of steps are run without computing averages, to let the system evolve far from the initial state, and the averages be independent of it. The rule to change the configuration α to α' from one step to the next is the simplest possible, i.e. reverse only one spin (so that the energy change between the two states involves only the nearest neighbours), and the probability that this state is effectively selected is:

$$P(\alpha \rightarrow \alpha') = 1 \text{ if } \Delta E = E\alpha' - E\alpha < 0$$

$$\text{and } P(\alpha \rightarrow \alpha') = \exp(-\beta\Delta E) \text{ otherwise}$$

In this manner, the system is always in a very probable state, with the probability corresponding exactly to the actual one. The averages can therefore be taken with equal weight for each of these states.

One big problem of this method, is that the successive states are not independent, but correlated, and the more so as we approach the critical point. If the states were quasi-independent, the noise on the computed averages will go down as $n_{step}^{-1/2}$, but in fact it goes down slower. The correlation time between configurations varies according to the correlation length ξ as

$$\tau = \xi^z$$

where z is a power close to 2. Near the critical point, where ξ diverges, there is a considerable slowing down of the method.

Other methods can cure this problem, such as the Swendsen-Wang algorithm or the Wolff method. The idea is to reverse blocks of spins simultaneously, from one step to the next, and to reduce existing correlations, in such a manner that existing clusters of aligned spins are broken in smaller clusters, or different clusters. The algorithm consists of linking all aligned spins by bonds, and so defining connected clusters. These bonds are then destroyed randomly, but with probability

$\exp(4\beta J)$. The smaller clusters resulting from this are re-oriented (up or down) randomly with equal probability. In some cases, it can be shown that the power z is then reduced to zero. In general computing the critical exponents through direct Monte-Carlo methods is not precise enough, and renormalization techniques are required.

5.4. RENORMALIZATION

Renormalization techniques were developed much earlier in quantum field theory (e.g. Gell-Mann & Low 1954), but their application in statistical physics awaited the 1970s (Wilson & Kogut 1974; Wilson 1975, 1983), although Kadanoff (1966) presented already ideas announcing how critical exponents could be extracted simply, with great intuition about the physical processes giving rise to critical phenomena.

The principle of a renormalization in real space (as opposed to conjugate space), is schematized in fig 3. In the transformation of renormalization, the scales are divided by a certain factor k , blocks of a certain number of sites (k^2) are replaced by one site, and since the system is scale-independent, we should be able to find an hamiltonian for the blocks which is of the same structure as the original one. The new system is less critical than the previous one, since the correlation length ξ has also been divided by k . It is a way to reduce the number of degrees of freedom of the system.

If the transformation of renormalization is called \mathbf{R} successive hamiltonians are related by

$$H_{n+1} = \mathbf{R}H_n$$

At each step, a similar hamiltonian must be found, with however different values of its parameters: coupling constant, temperature, etc..

The fixed points of the transformation, which obey

$$H = \mathbf{R}H$$

can be of various nature: attractive or repulsive (or mixed). They are attractive when after several iterations, neighbouring points are trapped there. In many problems, there exist trivial points, in the asymptotic regimes of low ($T \rightarrow 0$) or high ($T \rightarrow \infty$) temperatures. But in between, there can exist fixed points, corresponding to the critical points ($T = T_c$).

To give a very simple example, let us renormalize the Ising $d = 1$ problem, which can be carried out easily (cf Lesne 1996). The renormalization transformation will consist in considering only the even-numbered sites, and drop the odd-numbered ones. The scale is then

divided by 2. The partition function can be written as:

$$Z = \sum_j \exp(K_0 s_{2j+1}(s_{2j} + s_{2j+2}))$$

It is easy to demonstrate, since the spins can take only the values +1 and -1, that:

$$\exp(K_0(s_3s_2 + s_3s_4)) = 2\exp(K_1)\exp(K_1s_2s_4)$$

Then the partition function is exactly of the same form as the original one, after the division by 2, with

$$th(K_1) = th^2(K_0)$$

(or $\exp(2K_1) = ch^2(K_0)$). Let us consider now the fixed points, where $K_1 = K_0$, i.e. $th(K) = 0$, or $th(K) = 1$. This arrives in the two extreme cases, $K \rightarrow 0$ and $K \rightarrow \infty$. K is in fact the product of the coupling constant J , and β . The first case corresponds, for a finite temperature, to zero coupling, that is a purely thermal system, paramagnetic only; at zero B there is no correlation, and the system is not critical. Since the transform of K in this region is $\sim K^2$, and ξ is divided by 2 at each transform, we can deduce $\xi(K) = 2\xi(K^2)$, and the behaviour $\xi(K) \propto 1/|\log(K)|$, i.e. $\xi \rightarrow 0$. The second fixed point corresponds to a zero temperature ($K \rightarrow \infty$). Then we can show that $\xi(K) \propto \exp(2K)$, so ξ diverges, with large correlations. The system is truly critical.

In the general case, it is quite complex to find the easiest way to build blocks, and the new hamiltonian. A possible way is to Monte-Carlo renormalize, i.e. represent the transformation matrix of \mathbf{R} as a statistical average on the several possible choices. The critical exponent is then the largest eigen value of this matrix.

5.5. MEAN FIELD APPROXIMATION

This simple method to resolve the problem consists, for the Ising model of ferromagnet as an example, to replace the action of the ensemble of spins on a particular site, by the mean magnetic field at this position (it is also independent of site by translational invariance). This gives approximately when the system becomes critical (in general T_c is over-estimated), and approximate values of the critical exponents that do not depend on the spatial dimensionality (more exact when the latter is large, or for infinite-range interactions). For the 3D Ising model ($d = 3$), the critical exponents can be determined numerically to: $\alpha = 0.107$, $\gamma = 1.239$, $\nu = 0.631$ and $\eta = 0.037$; while in the mean field theory α

$= 0$, $\gamma = 1$, $\nu = 0.5$ and $\eta = 0$; the approximation appears therefore relatively bad.

5.6. FUNCTIONAL INTEGRALS

To efficiently use the renormalization methods, it is fruitful to go back to the field theory, domain in which the renormalization was first introduced, and numerous techniques are available. For example, in the case of the system of spins in a discrete lattice s_i , the discrete configurations of the lattice are replaced by a continuous field $s(\vec{x})$. The summation on the sites Σ_i are replaced by spatial integrals $\int d\vec{x}$; the hamiltonian becomes a functional of the field $s(\vec{x})$,

$$H(s, T) = \beta \int A(\vec{s}, \vec{x}) d\vec{x}$$

The summation over various configurations, to obtain for instance the partition function Z , is replaced by a functional integral, of variable the field $s(\vec{x})$:

$$Z = \int_{\vec{s}} \exp(-H(\vec{s}, T))$$

Often the calculations are more easy in the Fourier conjugate space, the renormalised hamiltonian H_1 is defined of the same form as the original one H_0 , as

$$\exp(H_1) = \int_{\phi} \exp(H_0(\Phi_0 + \phi))$$

The renormalised hamiltonian H_1 can be expressed as a perturbative development, with the help of a diagrammatic analysis.

6. Statistical Self-Gravity

As was shown in section 4, it appears that the self-gravitating system is critical for a large range of the parameters, and it is difficult to isolate a critical point, to identify diverging behaviours. However, it is well known (Wilson 1975, Domb & Green 1976), that physical quantities diverge only for infinite volume systems, at the critical point. Since our systems are also finite and bounded, they only approach asymptotically the divergences.

6.1. IDENTIFICATION OF THE FRACTAL DIMENSION

If Λ measures the distance to the critical point, (in spin systems for instance, Λ is proportional to $|T - T_c|$), the correlation length ξ diverges as,

$$\xi(\Lambda) \sim \Lambda^{-\nu}$$

and the specific heat (per unit volume) \mathcal{C} as,

$$\mathcal{C} \sim \Lambda^{-\alpha}$$

But in fact, for a finite volume system, all physical quantities are finite at the critical point. When the typical size R of the system is large, the physical magnitudes take large values at the critical point, and the infinite volume theory is used to treat finite size systems at criticality. In particular, for our system, the correlation length provides the relevant physical length $\xi \sim R$, and we can write

$$\Lambda \sim R^{-1/\nu}$$

Our system has the symmetries $d = 3$ and $D = 1$ (scalar field), which should indicate the universality class to which it corresponds. It remains to identify the corresponding operators. Already in the previous sections, it was suggested that the field ϕ corresponds to the potential, and the mass density

$$m \rho(\vec{x}) = m e^{\phi(\vec{x})}$$

can be identified with the energy density in the renormalization group (also called the ‘thermal perturbation operator’).

We note that the state of zero density (or zero fugacity), corresponds to a singular point, around which we develop the physical functions (and we choose Λ accordingly). At this point $\mu^2/T_{eff} = 0$, the partition function \mathcal{Z} is singular

$$\Lambda \equiv \frac{\mu^2}{T_{eff}} = z \left(\frac{2\pi m k T}{h^2} \right)^{3/2}$$

i.e., the critical point $\Lambda = 0$ corresponds to zero fugacity z . We can write \mathcal{Z} as a function of the action S^* at the critical point

$$\mathcal{Z}(\Lambda) = \int \int \mathcal{D}\phi e^{-S^* + \Lambda \int d^3x e^{\phi(\vec{x})}}$$

Let us now decompose $\log \mathcal{Z}$ in its singular and regular parts (we know that the second derivative will give the heat capacity that diverges in $\Lambda^{-\alpha}$)

$$\frac{1}{V} \log \mathcal{Z}(\Lambda) = \frac{K}{(2-\alpha)(1-\alpha)} \Lambda^{2-\alpha} + F(\Lambda)$$

where $F(\Lambda)$ is an analytic function of Λ around the origin

$$F(\Lambda) = a \Lambda + \frac{1}{2} b \Lambda^2 + \dots$$

$V = R^3$ stands for the volume and K , a and b are constants.

By derivation with respect to Λ

$$\frac{1}{V} \frac{\partial}{\partial \Lambda} \log \mathcal{Z}(\Lambda) = a + \frac{K}{1-\alpha} \Lambda^{1-\alpha} + \dots = \frac{1}{V} \int d^3x \langle e^{\phi(\vec{x})} \rangle$$

Now, using the standard relation $\alpha = 2 - \nu d = 2 - 3\nu$, this gives

$$\frac{\partial}{\partial \Lambda} \log \mathcal{Z}(\Lambda) = V a + \frac{K}{1-\alpha} R^{1/\nu} + \dots$$

The mass contained in a region of size R is

$$M(R) = m \int^R e^{\phi(\vec{x})} d^3x$$

$$\langle M(R) \rangle = m V a + m \frac{K}{1-\alpha} R^{1/\nu} + \dots$$

We already see that, apart a possible constant density, the average mass obeys a singular power-law.

The 2-points density correlator varies as

$$C(\vec{r}_1, \vec{r}_2) \sim |\vec{r}_1 - \vec{r}_2|^{\frac{2}{\nu}-6}$$

The perturbative calculation matches with this result for $\nu = \frac{1}{2}$, the mean field value for the exponent ν . Pursuing further to the second derivative of $\log \mathcal{Z}(\Lambda)$ with respect to Λ

$$\frac{\partial^2}{\partial \Lambda^2} \log \mathcal{Z}(\Lambda) = V [\Lambda^{-\alpha} K + b + \dots]$$

$$\frac{\partial^2}{\partial \Lambda^2} \log \mathcal{Z}(\Lambda) = \int d^3x d^3y C(\vec{x}, \vec{y}) \sim R^D \int^R \frac{d^3x}{x^{6-2d_H}} \sim \Lambda^{-2} \sim R^D \Lambda^{-\alpha}$$

we can find the mass fluctuations and corresponding dispersion:

$$(\Delta M(R))^2 \equiv \langle M^2 \rangle - \langle M \rangle^2 \sim \int d^3x d^3y C(\vec{x}, \vec{y}) \sim R^{2/\nu}$$

$$\Delta M(R) \sim R^{1/\nu}$$

This is the definition relation of the fractal, with dimension d_H , and the scaling exponent ν can be identified with the inverse Hausdorff dimension of the system

$$d_H = \frac{1}{\nu}$$

The velocity dispersion follows

$$\Delta v \sim R^q$$

with

$$q = \frac{1}{2} \left(\frac{1}{\nu} - 1 \right) = \frac{1}{2} (d_H - 1)$$

6.2. NUMERICAL VALUES

The scaling exponents ν , α can be computed through the renormalization group approach. The case of a single component (scalar) field has been extensively studied in the literature (Hasenfratz & Hasenfratz 1986, Morris 1994a,b). Very probably, there is a unique, infrared stable fixed point in 3D: the Ising model fixed point. Such non-perturbative fixed point is reached in the long scale regime independently of the initial shape of the interaction (ϕ). For the Ising model $d = 3$, the exponents are: $\nu = 0.631$, from which we deduce $d_H = 1.585$, $\eta = 0.037$, and $\alpha = 0.107$.

The value of the dimensionless coupling constant $g^2 = \mu T_{eff}$ should decide whether the fixed point chosen by the system is the mean field (weak coupling) or the Ising one (strong coupling). At the tree level, we estimate $g \approx \frac{5}{\sqrt{N}}$, where N is the number of points in a Jeans volume d_J^3 . The coupling constant appears then of the order of 1, and we cannot settle this question without effective computations of the renormalization group equations. In any case, both the Ising and mean field values are in agreement with the astronomical observations (the mean field exponents are $\nu = 0.5$, $d_H = 2$, $\eta = 0$ and $\alpha = 0$).

6.3. IMPORTANT DIFFERENCES WITH THE SPIN MODELS

For the gravitational gas we find scaling behaviour for a full range of temperatures and couplings, while for spin models scaling only appears at the critical value of the temperature. At $T = T_c$, the correlation length ξ is infinite, and the theory is massless. In fact, since the spin systems are not infinite, even in the critical domain, ξ is finite and the correlation functions decrease as $\sim e^{-r/\xi}$ for large distances r (only ξ

is large, of the order of the system size). Fluctuations of the relevant operators support perturbations which can be interpreted as massive excitations.

Such (massive) behaviour does not appear for the gravitational gas. The density correlators scale, exhibiting power-law behaviour. This feature is connected with the scale invariant character of the Newtonian force and its infinite range.

6.4. OBSERVATIONAL TESTS

It was shown that the predicted fractal dimension of a self-gravitating critical medium is compatible with that of the astrophysical applications (interstellar medium, galaxies), within the observational uncertainties. However, there are other predictions of the theory, that could be checked. It is well known in critical phenomena that there exists two independent critical exponents: the second one concerns the correlations of the potential, corresponding to the field ϕ

$$\langle \phi(\vec{r})\phi(0) \rangle \sim r^{-1-\eta}$$

The potential is then predicted to vary as a power law with size, with a slope $-1/2 - \eta/2 = -0.518$. It is not easy to observe directly this quantity, but tracers of the potential could be obtained through light rays that are deviated by astrophysical masses. As for the ISM, for example, the potential fluctuations could be traced by the micro-lensing produced on the light of remote quasars, while they are crossing the ISM of intervening galaxies, at high redshift. Time fluctuations of the quasars flux is regularly observed, and interpretation in terms of micro-lensing has been proposed (Lewis et al 1993).

7. Conclusion

We have emphasized the existence of two astrophysical fractals, the interstellar medium, with structures ranging from 10 AU to 100 pc, and the large-scale structures of galaxies, from 50 kpc to 150 Mpc at least. The first one is in statistical equilibrium, while the second one is still growing to larger scales. In both cases, we can describe these media as developing large-scale fluctuations with large correlations as is familiar in critical phenomena. We propose that in both cases, self-gravity is the main force governing these fractal structures.

The statistical thermodynamic approach is developed, and it is shown that the phenomenological potential, which is in $1/r$ between

two cutoffs (at small and large-scale), can be described by a scalar field theory. We use the renormalization group methods for this scale-independent system, to find the universality class of the problem. The fractal dimension, and the potential correlations exponent can be derived from the critical exponents of the Ising $d = 3$ model. The stability of the results with respect to perturbations has been studied; the results are quite robust with respect to perturbations of external forces. Of course, if the external energy is large with respect to the self-gravitational energy of the gas (in the vicinity of violent star-formation in the ISM for instance), then the hierarchical structure will be destroyed. The observed fractal dimensions are compatible with the predictions, and other observational tests are proposed.

References

- Abell G.O.: 1958, ApJS 3, 211
 Balian R., Schaeffer R.: 1988, ApJ 335, L43
 Balian R., Schaeffer R.: 1989, A&A 226, 373
 Bazell D., Desert F.X.: 1988, ApJ 333, 353
 Binney J.J., Dowrick N.J., Fisher A.J., Newman M.E.J.: 1992 ‘The Theory of Critical Phenomena’, Oxford Science Publication.
 Bond J.R., Cole S., Efstathiou G., Kaiser N.: 1991, ApJ 379, 440
 Bouchet F.R., Schaeffer R., Davis M.: 1991, ApJ 383, 19
 Brand P., Wouterloot J.G.: 1995, A&A ???
 Casoli F., Combes F., Gerin M.: 1984, A&A 133, 99
 Castagnoli C., Provenzale A.: 1991, A&A 246, 634
 Cole S., 1989, PhD Thesis, Univ. of Cambridge
 Coleman P.H., Pietronero L., Sanders R.H.: 1988, A&A 200, L32
 Coleman P.H., Pietronero L.: 1992, Phys. Rep. 231, 311
 Colombi S., Bouchet F.R., Hernquist L.: 1996, ApJ 465, 14
 Combes F., Pfenniger D.: 1997, A&A 327 453
 Dame T.M., Elmegreen B.G., Cohen R.S., Thaddeus P.: 1986, ApJ 305, 982
 Davis M.A., Meiksin M.A., Strauss L.N., da Costa and Yahil A.: 1988, ApJ 333, L9
 Davis M.A.: 1997 in ‘Critical Dialogs in Cosmology’, ed. N. Turok, astro-ph/9610149
 Davis M.A., Peebles P.J.E.: 1977, ApJS 34, 425
 Davis M.A., Peebles P.J.E.: 1983, ApJ 267, 465
 Davis R.J., Diamond P.J., Goss W.M.: 1996, MNRAS 283, 1105
 de Vaucouleurs G.: 1960, ApJ 131, 585
 de Vaucouleurs G.: 1970, Science 167, 1203
 de Vega H., Sánchez N., Combes F.: 1996a, Nature 383, 53
 de Vega H., Sánchez N., Combes F.: 1996b, Phys. Rev. D54, 6008
 de Vega H., Sánchez N., Combes F.: 1998, ApJ in press
 Diamond P.J., Goss W.M., Romney J.D. et al: 1989, ApJ 347, 302
 Di Nella H., Montuori M., Paturel G., Pietronero L., Sylos Labini F.: 1996, A&A 308, L33
 Domb C., Green M.S.: 1976, ‘Phase transitions and Critical Phenomena’, vol. 6, Academic Press

- Dubrulle B., Lachièze-Rey M.: 1994, *A&A* 289, 667
 Falconer K.J.: 1990, *Fractal geometry*, Wiley, Chichester
 Falgarone, E., Phillips, T.G., Walker, C.K.: 1991, *ApJ* 378, 186
 Falgarone, E., Lis D.C., Phillips, T.G. et al: 1994, *ApJ* 436, 728
 Fleck R.C.: 1981, *ApJ* 246, L151
 Fiedler R.L., Dennison B., Johnston K., Hewish A.: 1987, *Nature* 326, 675
 Fiedler R.L., Pauls T., Johnston K., Dennison B.: 1994, *ApJ* 430, 595
 Gell-Mann M., Low F.E.: 1954, *Phys. Rev.* 95, 1300
 Hamilton A.J.S.: 1993, *ApJ* 417, 19
 Hasenfratz P., 1986, *Nucl.Phys.* B270, 687
 Heithausen A.: 1996, *A&A* 314, 251
 Heithausen A., Bensch F., Stutzki J., Fakgarone E., Panis J.F.: 1998, *A&A* 331, L65
 Horwitz G., Katz J., 1978a, *ApJ* 222, 941
 Horwitz G., Katz J., 1978b, *ApJ* 223, 311
 Houlahan P., Scalo J.: 1992, *ApJ* 393, 172
 Hoyle F.: 1953, *ApJ* 118 513
 Hubbard J., 1959, *Phys. Rev. Lett.* 3, 77
 Inutsuka S-I., Miyama S.M.: 1997, *ApJ* 480 681
 Itoh M., Inagaki S., Saslaw W.C.: 1993, *ApJ* 403, 459
 Kadanoff L.P.: 1966 *Physics* 2, 263
 Kolmogorov A.: 1941, in "Compt. Rend. Acad. Sci. URSS" 30, 301
 Lacey C.G., Cole S.: 1993, *MNRAS* 262, 627
 Lacey C.G., Cole S.: 1994, *MNRAS* 271, 676
 Lachièze-Rey M.: 1993, *ApJ* 407, 1 & *ApJ* 408, 403
 Larson R.B., 1981, *MNRAS* 194, 809
 Larson R.B., 1985, *MNRAS* 214, 379
 Lewis G.F., Miralda-Escude J., Richardson D.C., Wambsganss J.: 1993, *MNRAS* 261, 647
 Lesne A.: 1996, in "Méthodes de renormalisation", Eyrolles Sciences
 Lin H. et al: 1996, *ApJ* 471, 617
 Magnani L., Blitz L., Mundy L. 1985, *ApJ* 295, 402
 Mandelbrot B.B.: 1975, 'Les objets fractals', Paris, Flammarion
 Mandelbrot B.B.: 1982, 'The fractal geometry of nature', New York: Freeman
 Martinez V.J., Paredes S., Saar E.: 1993, *MNRAS* 260, 365
 McLaughlin D.E. & Pudritz R.E.: 1996, *ApJ* 469, 194
 Miesch M., & Scalo J.M.: 1995, *ApJ* 450, L27
 Morris T.R., 1994a: *Phys. Lett.* B329, 241
 Morris T.R., 1994b: *Phys. Lett.* B334, 355
 Myers P.C.: 1983, *ApJ* 270, 105
 Ostriker J.P.: 1993, *ARAA* 31, 689
 Padmanabhan 1990, *Phys. Rep.* 188, 285
 Parisi G.: 1988, 'Statistical field theory', Addison Wesley, Redwood City
 Peebles P.J.E.: 1980, 'The Large-scale structure of the Universe', Princeton Univ. Press
 Peebles P.J.E.: 1993, 'Principles of physical cosmology' Princeton Univ. Press
 Pfenniger D., Combes F., Martinet L.: 1994, *A&A* 285 79
 Pfenniger D., Combes F.: 1994, *A&A* 285, 94
 Pietronero L., Montuori M., Sylos Labini F.: 1997, in 'Critical Dialogs in Cosmology', ed. N. Turok, astro-ph/9611197
 Pietronero L.: 1987, *Physica A*, 144, 257
 Postman M., Geller M.J., Huchra J.P.: 1986, *AJ* 91, 1267

- Postman M., Huchra J.P., Geller M.J.: 1992, ApJ 384, 404
Press W.H., Schechter P.: 1974, ApJ 187 425
Rees M.J.: 1976, MNRAS 176, 483
Saslaw W.C., Fang F.: 1996, ApJ 460, 16
Saslaw W.C., Hamilton A.J.S.: 1984, ApJ 276, 13
Scalo J.M.: 1985, in *Protostars and Planets II*, ed. D.C. Black & M.S. Matthews, Univ. of Arizona Press, Tucson, p. 201
Scalo J.M., 1987 in 'Interstellar Processes', D.J. Hollenbach and H.A. Thronson Eds., D. Reidel Pub. Co, p. 349
Scalo J.M., Lazarian A.: 1996, ApJ 469, 189
Schechter P.L.: 1976, ApJ 203, 297
Scott E.L., Shane S.D., Swanson M.D.: 1954, ApJ 119, 91
Shandarin S.F., Zel'dovich Ya. B.: 1989, Rev. Mod. Phys. 61, 185
Shapiro P.R., Kang H.: 1987, ApJ 318 32
Shapley H.: 1934, MNRAS 94, 791
Sheth R.K., Saslaw W.C.: 1996, Apj 470, 78
Smoot G., et al: 1992, ApJ 396, L1
Solomon P.M., Rivolo A.R., Barrett J.W., Yahil A.: 1987, ApJ 319, 730
Soneira R.M., Peebles P.J.E.: 1978, AJ 83, 845
Sreenivasan K.R., & Méneveau C.: 1986, J. Fluid Mech. 173, 357
Stratonovich R.L., 1958, Doklady, 2, 146
Sylos Labini F., Amendola L.: 1996, ApJ 438, L1
Sylos Labini F., Gabrielli A., Montuori M., Pietronero L.: 1996, Physica A 226, 195
Sylos Labini F., Pietronero L.: 1996, ApJ 469, 26
Sylos Labini F.: 1994, ApJ 433, 464
Toomre A.: 1964, ApJ 139, 1217
Totsuji H., Kihara T.: 1969; PASJ 21, 221
Vazquez-Semadeni E.: 1994, ApJ 423, 681
Vazquez-Semadeni E., Ballesteros-Paredes J., Rodriguez L.F.: 1997, ApJ 474, 292
Vazquez-Semadeni E., Canto J., Lizano S.: 1998, ApJ 492, 596
Uehara H., Susa H., Nishi R., Yamada M., Nakamura T.: 1996, ApJ 473 L95
Vergassola M., Dubrulle B., Frisch U., Noullez A.: 1994, A&A 289, 325
Vogelaar M.G.R., Wakker B.P.: 1994, A&A 291, 557
White S.D.M., Rees M.J.: 1978, MNRAS 183 341
White S.D.M.: 1979, MNRAS 186, 145
White S.D.M., Kauffmann G.: 1994, in "The formation and evolution of galaxies", V Canary Islands Winter School, ed. C. Munoz-Tunon & F. Sanchez, p. 455
Wilson K.G., Kogut, J.: 1974, Phys. Rep. 12, 75
Wilson K.G.: 1975, Rev. Mod. Phys. 47, 773
Wilson K.G.: 1983, Rev. Mod. Phys. 55, 583
Zamalodchikov A.B. 1989, Int. J. Mod. Phys. A4, 4235
Zel'dovich Ya. B.: 1970, Astrofizika 6, 319
Zinn-Justin J.: 1989, 'QFT and Critical Phenomena', Clarendon Press, Oxford

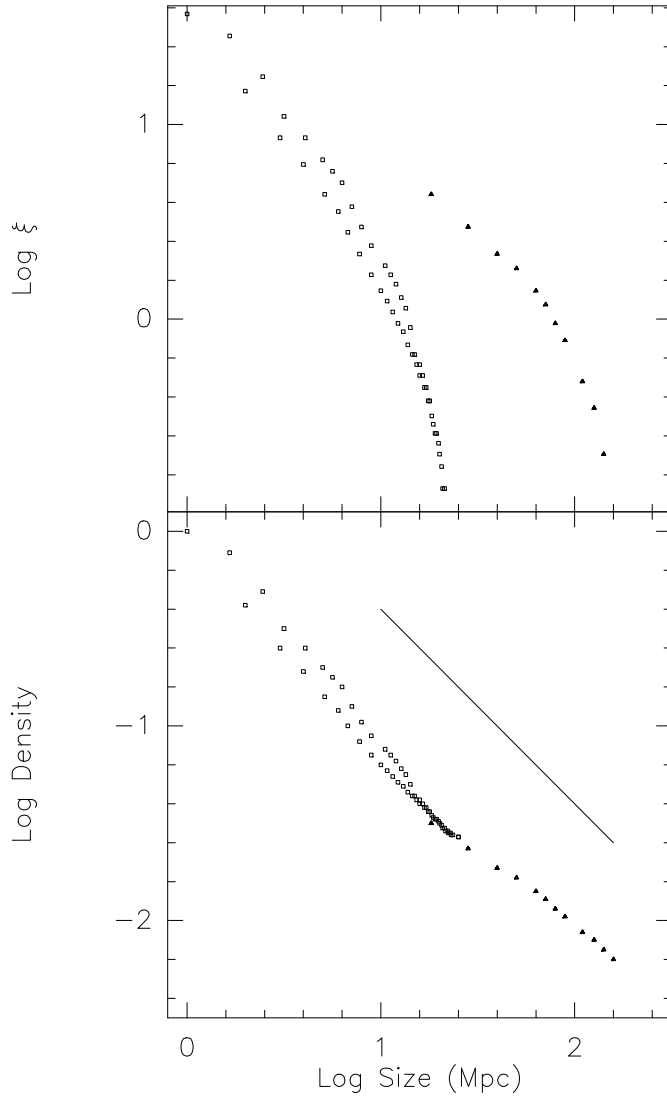


Figure 2. *Bottom:* the average conditional density $\Gamma(r)$ for several samples (Perseus-Pisces and CfA1 in open rectangles, and LEDA in filled triangles, adapted from Sylos-Labini & Pietronero 1996). *Top:* $\xi(r)$ corresponding to the same surveys. The indicative line has a slope $\gamma = 1$ (corresponding to a fractal dimension $D \sim 2$). This shows that it is difficult to determine the slope on the $\xi(r)$ function.

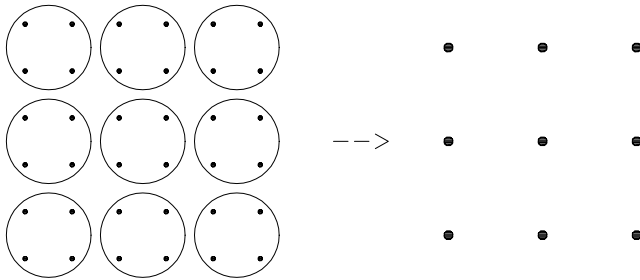


Figure 3. Renormalization of a square lattice. Blocks of 4 sites are replaced by one, dividing all scales by 2.